The *Arabidopsis* TRM1–TON1 Interaction Reveals a Recruitment Network Common to Plant Cortical Microtubule Arrays and Eukaryotic Centrosomes [C][W]

Stéphanie Drevensek,[a,1,2] Magali Goussot,[a,1] Yann Duroc,[a] Anna Christodoulidou,[a,3] Sylvie Steyaert,[a,4] Estelle Schaefer,[a] Evelyne Duvernois,[a,2] Olivier Grandjean,[a] Marylin Vantard,[b] David Bouchez,[a,5] and Martine Pastuglia[a]

[a] Institut Jean-Pierre Bourgin, Unité Mixte de Recherche 1318, Institut National de la Recherche Agronomique–AgroParisTech, Institut National de la Recherche Agronomique, Centre de Versailles, F-78000 Versailles, France
[b] Institut de Recherches en Technologies et Sciences pour le Vivant, Commissariat à l'Energie Atomique/Centre National de la Recherche Scientifique/Institut National de la Recherche Agronomique/Université Joseph Fourier, 38054 Grenoble, France

Land plant cells assemble microtubule arrays without a conspicuous microtubule organizing center like a centrosome. In *Arabidopsis thaliana*, the TONNEAU1 (TON1) proteins, which share similarity with FOP, a human centrosomal protein, are essential for microtubule organization at the cortex. We have identified a novel superfamily of 34 proteins conserved in land plants, the TON1 Recruiting Motif (TRM) proteins, which share six short conserved motifs, including a TON1-interacting motif present in all TRMs. An archetypal member of this family, TRM1, is a microtubule-associated protein that localizes to cortical microtubules and binds microtubules in vitro. Not all TRM proteins can bind microtubules, suggesting a diversity of functions for this family. In addition, we show that TRM1 interacts in vivo with TON1 and is able to target TON1 to cortical microtubules via its C-terminal TON1 interaction motif. Interestingly, three motifs of TRMs are found in CAP350, a human centrosomal protein interacting with FOP, and the C-terminal M2 motif of CAP350 is responsible for FOP recruitment at the centrosome. Moreover, we found that TON1 can interact with the human CAP350 M2 motif in yeast. Taken together, our results suggest conservation of eukaryotic centrosomal components in plant cells.

INTRODUCTION

Plant microtubule arrays display diverse patterns involved in cell division and division plane positioning, as well as in cell growth and in the direction of cell expansion. In plants, interphase microtubule arrays are positioned just beneath the plasma membrane through close interactions with the cell cortex, in a banded pattern organized transversely to the cell growth axis in rapidly elongating cells (Ehrhardt and Shaw, 2006; Wasteneys and Ambrose, 2009). At the onset of mitosis, during late G2, the cortical cytoskeleton undergoes a remarkable transformation where microtubules at the cortex are progressively depolymerized, except for a ring of microtubules encircling the nucleus. This preprophase band (PPB) of microtubules corresponds to a conspicuous, premitotic cytological landmark of the final division plane, predicting with exquisite precision the cortical site where the new cell plate will eventually attach upon completion of cytokinesis (Mineyuki, 1999; Müller et al., 2009; Duroc et al., 2010). The PPB disassembles in late prophase, progressively replaced by an acentriolar, anastral mitotic spindle during metaphase and anaphase. At late anaphase, the phragmoplast, a double-ring-shaped structure of microtubules and microfilaments responsible for the deposition of the new cell plate between daughter nuclei through vesicle transport, is formed. Starting from a central position, the phragmoplast grows centrifugally to reach the cortical site previously occupied by the PPB, eventually connecting to the membrane at this very position (Van Damme et al., 2007). As daughter cells enter G1, microtubules recolonize the cell periphery to establish the interphase cortical array, which participates in the control of cell elongation and drives cell wall deposition (Paradez et al., 2006; Lloyd and Chan, 2008).

Unlike many other eukaryotes, cells of land plants are devoid of a discrete microtubule organizing center (MTOC) like a centrosome, with the exception of basal bodies present in flagellate sperm cells of basal land plants that rely on aqueous fertilization. The way microtubule arrays are formed in the absence of a MTOC is still debated, although the involvement of γ-tubulin in nucleation processes has been clarified (Murata et al., 2005; Binarová et al., 2006; Pastuglia et al., 2006). Nucleation sites are spread over the cortex (Murata et al., 2005; Ehrhardt and Shaw, 2006), the nuclear surface (Stoppin et al., 1994) and the spindle

poles (Chan et al., 2003). Several authors hypothesize a diffuse and flexible MTOC at the cortex (Mazia, 1984; Chan et al., 2003), but very little information is available as to whether plant cells have retained, reorganized, or reinvented functions associated with MTOCs in other eukaryotes.

Apart from proteins of the bona fide γ-tubulin complex (Liu et al., 1994; Erhardt et al., 2002; Binarová et al., 2006; Pastuglia et al., 2006; Nakamura and Hashimoto, 2009; Kong et al., 2010), only a handful of plant proteins with similarity with animal centrosomal proteins have been identified and characterized (Pastuglia and Bouchez, 2007). In *Arabidopsis thaliana*, this includes NEDD1 (Zeng et al., 2009), Cyclin-Dependent Kinase A;1 (Weingartner et al., 2004), FASS/TONNEAU2 (TON2) (Camilleri et al., 2002), and TON1 (Azimzadeh et al., 2008). In *Arabidopsis*, NEDD1, which acts as an anchoring factor of γ-tubulin complex to the centrosome in human cells (Manning and Kumar, 2007), decorates spindle and phragmoplast microtubules preferentially toward theirs minus ends and plays a critical role in microtubule organization during mitotic cell division (Zeng et al., 2009). In animal cells, CDKA is activated in early prophase at the centrosome (Jackman et al., 2003). In *Arabidopsis*, it is recruited at the same stage to the late PPB (Weingartner et al., 2004). The *FASS/TON2* gene encodes a Protein Phosphatase2A (PP2A) regulatory subunit (Camilleri et al., 2002) similar to the *Caenorhabditis elegans* RSA-1 protein, which is involved in the recruitment of a PP2A complex at the centrosome (Schlaitz et al., 2007). TON1 proteins are small acidic proteins highly conserved in land plants, and they interact with centrin, a major constituent of eukaryotic MTOCs (Azimzadeh et al., 2008). The N terminus of TON1 shares sequence similarity with FGFR1 Oncogen Partner (FOP), a human centrosomal protein originally identified from a human myeloproliferative syndrome (Popovici et al., 1999; Andersen et al., 2003; Lelièvre et al., 2008). FOP is recruited to the centrosome through its interaction with Centrosome-Associated Protein350 (CAP350), a large centrosomal protein suspected to be involved in microtubules anchoring at the centrosome of human cells (Yan et al., 2006). CAP350 has also been proposed to specifically stabilize Golgi-associated microtubules, participating in the maintenance of a continuous pericentrosomal Golgi ribbon (Hoppeler-Lebel et al., 2007).

The *ton1* and/or *fass* mutations have been studied in *Arabidopsis*, maize (*Zea mays*), and *Physcomitrella patens*. In *Arabidopsis*, *TON1* and *FASS* loss of function induces the same phenotype: Seedlings are dwarf and stunted and display abnormal cell elongation and random positioning of mitotic division planes (Torres-Ruiz and Jürgens, 1994; Traas et al., 1995). The organization of cortical microtubule arrays is strongly perturbed in mutant cells: In interphase, microtubules lose the parallel transverse organization typical of wild-type cells, and PPBs are never observed in premitotic mutant cells (Traas et al., 1995; Camilleri et al., 2002; Azimzadeh et al., 2008). The *Arabidopsis ton1* and *fass* mutants are the only viable plant mutants unable to form a PPB. In maize, the two *FASS* homologs (*Discordia1* [*DCD1*] and *Alternative Discordia1* [*ADD1*]) appear essential, and double homozygote plants are never recovered (Wright et al., 2009). *add1* mutants have no phenotype, whereas the *DCD1* mutation affects orientation of cell division plane during asymmetric divisions in the leaf epidermis (Wright et al., 2009). Loss of function of *P. patens TON1* strongly affects development of the

moss gametophore, phenocopying the developmental syndrome observed in *Arabidopsis ton1* mutants and confirming the dual function of *TON1* in organizing cortical arrays of microtubules during both interphase and premitosis (Spinner et al., 2010). Localization studies have shown that TON1 is associated with the cortical cytoskeleton and labels the PPB in *Arabidopsis* (Azimzadeh et al., 2008). The FASS homologs in maize, DCD1 and ADD1, colocalize with the PPB and remain at the cortical division site through metaphase (Wright et al., 2009).

To get further insights into TON1 function, we searched for TON1 protein partners. Here, we describe the characterization of a new superfamily of 34 *Arabidopsis* proteins that are able to interact with TON1 and are found only in plants. The TON1 Recruiting Motif (TRM) superfamily is defined by the presence of six short shared sequence motifs always found in a conserved order on primary sequences. An archetypal member of the family, TRM1, was chosen for further analysis and was shown to localize to cortical microtubules arrays in *Arabidopsis* cells and to bind microtubules in vitro. Likewise, several, but not all, members of the TRM family decorate microtubule arrays in tobacco (*Nicotiana benthamiana*) cells. Moreover, we show that TRM1 is able to recruit TON1 to the cytoskeleton through its C-terminal M2 motif. Three motifs of TRMs are also present in the human centrosomal protein CAP350 in the same order as in TRMs. In CAP350, a C-terminal M2-like motif is responsible for FOP recruitment at the centrosome and interacts with *Arabidopsis* TON1 in yeast.

RESULTS

TON1 Two-Hybrid Interactants Define a New Family of Plant Proteins

To identify TON1 protein partners, the full-length TON1 protein was used as bait in a two-hybrid interaction screen in yeast. From 250 clones isolated, ~10% originated from an *Arabidopsis* centrin gene (CEN1; At3g50360), as previously described (Azimzadeh et al., 2008), and 2% from a proteasome subunit. Twelve other two-hybrid interactants, representing 66% of the clones, were isolated from the screen (see Supplemental Table 1 online). One to four independent clones of different sizes were recovered per putative interactant. In all cases, these clones harbored C-terminal fragments of various size from large *Arabidopsis* proteins. Sequence analysis of the recovered C-terminal regions showed that they all share partial sequence similarity. These proteins were named TRMs. The smallest interacting clone corresponded to the last 79 residues of At3g02170 (hereafter TRM1). TRM1 was the most abundant interactant recovered (11% of total) and was represented by four independent clones ranging from 79 to 149 C-terminal residues. The second most represented gene was At5g15580 (hereafter TRM2), which is 72% similar to TRM1 in protein sequence. It accounts for 10% of the clones, with three independent clones ranging from 139 to 393 C-terminal residues.

To map regions involved in interaction between TRM proteins and TON1, truncated versions of TRM1 were cloned into two-hybrid vectors and confronted for interaction with TON1 in yeast
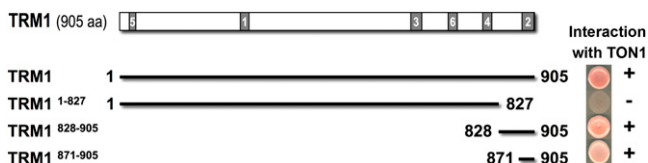
Figure 1. The Last 33 C-Terminal Residues of TRM1 Are Sufficient for Interaction with TON1.

Summary of TRM1–TON1 interactions as determined by yeast two-hybrid analyses between TRM1 fragments and full-length TON1. Growth on selective medium was visually noted from no significant growth (−) to full-growth (+). The numbered boxes in the TRM1 protein depicted at the top designate the M1-M6 motifs. aa, amino acids.
[See online article for color version of this figure.]

(Figure 1). This revealed that the two full-length proteins are able to interact in yeast and confirmed that the last 79 residues of TRM1 are necessary and sufficient for interaction with TON1. Further deletion of TRM1 showed the last 33 C-terminal residues are sufficient for interaction with TON1 in yeast (Figure 1).

TRM Proteins Share Six Conserved Sequence Motifs

Multiple alignment of the 12 two-hybrid TRMs detected small stretches of similarity shared by all sequences. The MEME tool was used to define those conserved motifs more precisely. The MEME-generated motifs were then used for scanning the *Arabidopsis* complete proteome (TAIR9) using the MAST algorithm; this identified a total of 33 *Arabidopsis* proteins with an E-value ≤ 0.5, including the 12 starting TRMs. The 12 two-hybrid TRMs were also used for standard BLAST similarity search against the predicted protein set of *Arabidopsis*. Altogether, the 12 TRMs identified 25 *Arabidopsis* proteins at a cutoff E-value of 10^{-3}. Sequences retrieved from MAST and BLAST were combined into a nonredundant set of 34 *Arabidopsis* proteins.

The 34 TRM proteins shared six highly significant sequence motifs disposed in the very same order along protein sequences (Figure 2; see Supplemental Figure 1 online). The motifs were from 17 to 25 residues in length, and their order along protein sequences was strictly conserved (M5-M1-M3-M6-M4-M2). All 34 TRMs contained motif M2 (25 amino acids) at the C terminus, plus one to five of the others, five TRMs containing all six. M5, M1, M3, M6, and M4 were present in 20, 21, 23, 21, and 21 TRMs, respectively (Figure 2). As all 34 TRMs possess a C-terminal M2 motif, we assume that the ability to interact with TON1 is not restricted to the 12 original two-hybrid TRMs but is likely a feature of the whole TRM superfamily.

Some TRMs showed sequence similarity outside of the conserved M1-6 motifs. Multiple alignment procedures followed by neighbor-joining phylogenetic analysis and bootstrap validation allowed us to define eight TRM groups of two to five members (Figure 2), plus a few isolated ones. Apart from the six motifs, no significant similarity is detectable between groups. TRMs are rather large (80 kD on average) and charged proteins, covering a large range of pI from 4.3 to 10.6. They often contain a large positively charged domain of 150 to 300 residues, followed by an acidic C-terminal region. Prediction algorithms do not give any

clue as to their subcellular targeting and function. Consistent with a role at the cell cortex, currently available *Arabidopsis* proteome data (Heazlewood et al., 2007) identify TRM7 as a plasma membrane–associated protein (Nühse et al., 2003), while TRM14 and TRM19 are found in cortex fractions (Benschop et al., 2007). Among the 34 TRM proteins, only TRM1, TRM2, and TRM29 have been studied before. TRM29 has been identified as a nuclear protein interacting with the ALCATRAZ transcription factor and was named ALCATRAZ-Interacting protein (Wang et al., 2008). TRM1 and TRM2 have been isolated previously in a genetic screen for leaf morphology defects, and the mutants were given the names *longifolia2* (*lng2*) and *lng1*, respectively (Lee et al., 2006).

Searches in sequence databases, either EST or genomic, identified a number of similar sequences in the plant kingdom, showing the occurrence of TRMs in land plants. *Arabidopsis* TRMs do not show significant similarity to any nonplant protein, nor do they show regions or motifs of known function. Using *Arabidopsis* motifs on available plant genomes, MAST searches revealed 34 TRM members in rice (*Oryza sativa*), seven in *Selaginella*, and 19 in *Physcomitrella*. There is no global one-to-one conservation of individual TRMs between *Arabidopsis* and rice, and orthology relationships are difficult to assess in the family. Nevertheless, the organization of the superfamily is comparable, and all *Arabidopsis* groups seem present in rice as paralogous groups. Although not a typical TRM, a large ~5000-residue coil-coiled protein containing C-terminal motifs M3-M4-M2 is present in the *Chlamydomonas/Volvox* genome (XP_001695911.1).

TRM1 Interacts with TON1 in Vivo

Since the TRM1 sequence possesses the six motifs defining the TRM family and is the most represented gene among the clones recovered from the two-hybrid screen, TRM1 was considered as an archetypal TRM and chosen for further analysis.

Transcriptomic analysis using the Genevestigator tool (Zimmermann et al., 2004) indicates that *TRM1* RNA accumulates predominantly in flowering tissues and to a lesser extent in leaves (see Supplemental Figure 2 online). We raised an antibody directed against two peptides of TRM1 defined in regions of minimal similarity with TRM2. On immunoblots, this antibody recognized a protein band of an apparent molecular mass of ~120 kD not present in the *TRM1* loss-of-function mutant allele (Lee et al., 2006), which confirmed its specificity toward TRM1 (Figure 3A). In addition, immunoblot analysis indicated that the TRM1 protein is more abundant in flowers and flower buds than in leaves (Figure 3A). This expression profile is in agreement with transcriptome data and with the phenotype induced by *lng2* (*trm1*) mutation that affects leaf, flower, and silique size (Lee et al., 2006).

To ascertain that TRM1 and TON1 interact in vivo under physiological conditions, we tested whether they were able to coprecipitate from protein extracts of a line expressing a genomic translational fusion between green fluorescent protein (GFP) and TON1 (GFP-gTON1). This construct encompasses a 7.4-kb genomic fragment that harbors the *TON1a* gene and 4.6 kb of promoter, with the GFP tag inserted at its N-terminal end.
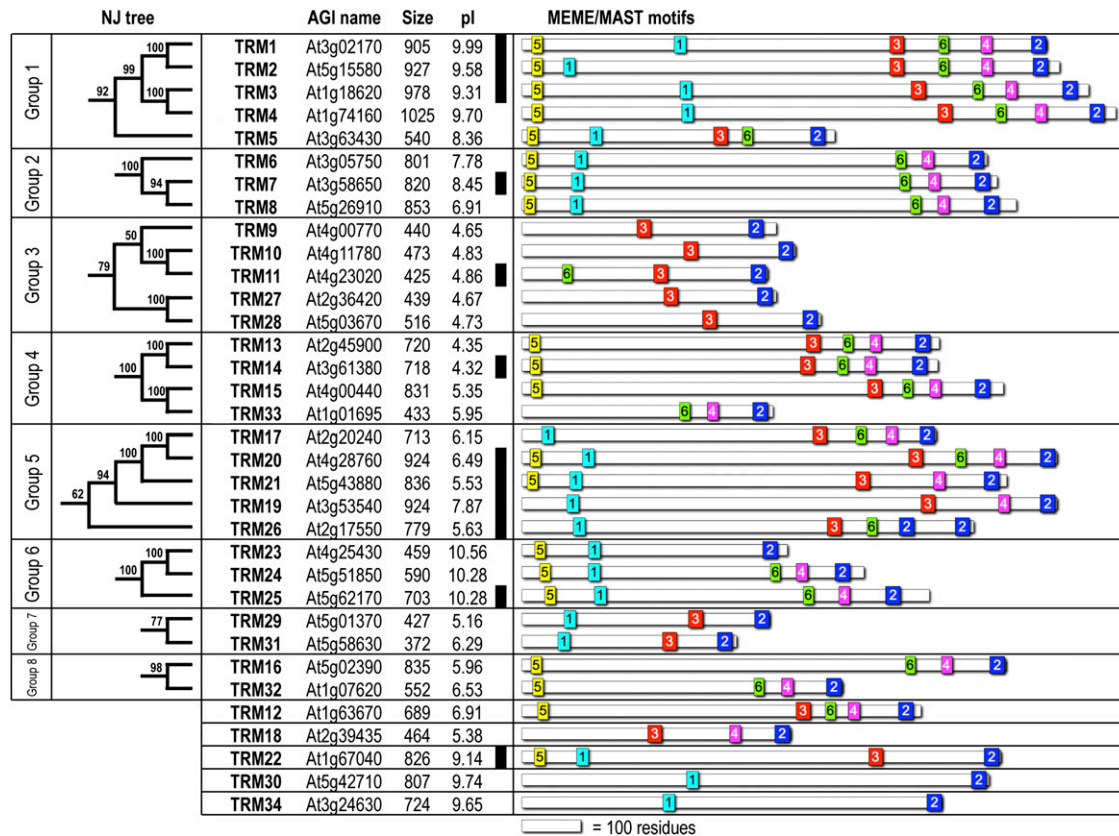
Figure 2. Six Motifs Define a Superfamily of 34 Proteins in *Arabidopsis*.

Maps of the 34 predicted TRM polypeptides, with occurrence and position of the motifs shown on the right. The eight groups of TRM proteins were defined by multiple alignment procedures, manually curated, and submitted to neighbor-joining phylogenetic analysis (unrooted NJ tree) and bootstrap validation (1000 trials); only strongly supported nodes are represented here (see Supplemental Data Set 1 online). The Arabidopsis Genome Initiative (AGI) gene number, calculated size (in residues), and pI of each predicted protein are indicated. Black bars indicate TRMs isolated from the two-hybrid screen using TON1 as bait.

[See online article for color version of this figure.]

Using the anti-TRM1 antibody, we showed that TRM1 copurified with GFP-TON1 in flower bud extracts, demonstrating that both proteins are able to interact in vivo (Figure 3B).

TRM1 Is a Microtubule-Associated Protein

To investigate the subcellular localization of TRM1, we fused GFP to its N terminus and expressed the fusion protein from its native promoter in *Arabidopsis* plants. Immunoblot analysis of transgenic lines revealed that the expression level of the GFP-TRM1 fusion is comparable to that of the native TRM1, and complementation studies showed that the ProTRM1:GFP-TRM1 construct is functional (see Supplemental Figure 3 online). In transgenic lines expressing the ProTRM1:GFP-TRM1 construct, GFP fluorescence was undetectable in roots, hypocotyls, or leaves but present, although very faint, in petal epidermal cells, where indeed maximal expression is expected from transcriptome data. The *Arabidopsis* petal consists of a basal greenish claw and a distal white blade and contains a single layer of epidermal cells overlying the mesophyll and vasculature. In the

blade, the epidermis contains conical cells (on the adaxial side) or rounded and cobblestone-like cells (on the abaxial side), whereas epidermal cells are more elongated in the claw. In young petals, GFP-TRM1 fluorescence aligned along filamentous structures in the cortical region of epidermal cells (Figures 4A and 4B). This linear (and somewhat punctate) pattern suggests an association of GFP-TRM1 with cortical microtubules. The observed patterns match the organization of cortical microtubules in such cell types: In elongating epidermal cells of the claw, parallel arrays perpendicular to the cell elongation axis (Figure 4C), contrasting with mixed orientation in conical and rounded epidermal cells of the blade (Figure 4D). Colocalization of GFP-TRM1 with microtubules was assessed in lines coexpressing GFP-TRM1 and an mCherry-β-tubulin6 microtubule marker (Nakamura et al., 2010). Although GFP-TRM1 signal was faint, there was a clear coalignment of GFP-TRM1 fluorescence with microtubules (Figures 4E and 4F).

To test whether TRM1 directly binds to microtubules, we performed in vitro microtubule cosedimentation assays using TRM1 produced in *Escherichia coli*. TRM1 was incubated with
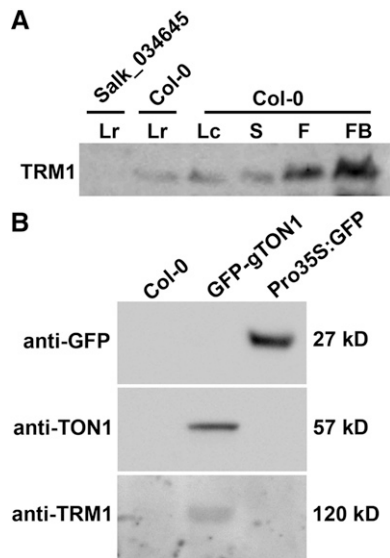
Figure 3. TRM1 Interacts with TON1 in Vivo.

(A) Immunoblot analysis of TRM1 protein levels in *Arabidopsis* tissues. Protein expression was tested in rosette leaves (Lr), cauline leaves (Lc), stem (S), opening flowers (F), and flower buds (FB) of Columbia-0 (Col-0) plants. Rosette leaves from the loss-of-function mutant allele *Salk_034645* (also named *lng2-2* in Lee et al., 2006) correspond to the negative control. **(B)** Coprecipitation experiments using GFP-trap beads were performed on flower buds extracts from Col-0 plants and from plants expressing GFP under the control of the 35S promoter or the genomic GFP-gTON1 fusion construct. Coprecipitated proteins were then analyzed by immunoblotting using the indicated antibodies. TRM1 is only copurified in coprecipitates of GFP-gTON1 extracts, demonstrating TRM1–TON1 interaction in vivo.

preformed taxol-stabilized microtubules. After sedimentation, the amounts of soluble and sedimented TRM1 were quantified by densitometry. Without microtubules, most TRM1 (98%) remained in the supernatant, whereas upon incubation with microtubules, 91% of TRM1 pelleted with microtubules (Figure 4G), demonstrating the ability of purified TRM1 to directly bind microtubules.

To map the region(s) of TRM1 involved in microtubule binding, a series of truncated fragments of TRM1 were fused with GFP in N- and C-terminal position (Figure 5). All constructs were transiently expressed in *Nicotiana benthamiana* leaves. From the 10 TRM1 fragments tested, five of them showed microtubule association (Figure 5B). Colocalization was confirmed by coexpressing TRM1 fragments fused to red fluorescent protein (RFP) and the microtubule marker GFP-α-tubulin6 (Figure 5C). The shortest fragment retaining the ability to bind microtubules mapped to residues 342 to 586 of TRM1. This region corresponds to a large basic domain of the protein (Figure 5A). The identification of the microtubule binding domain was further confirmed by an in vitro cosedimentation assay. When the purified TRM1$^{342-586}$ fragment expressed in *E. coli* was centrifuged in the absence of microtubules, 77% of the protein remained in the supernatant. Conversely, when the TRM1$^{342-586}$ fragment was incubated with microtubules, 99% of the TRM1$^{342-586}$ pool was recovered in the pellet (Figure 5D).

Not All TRM Proteins Are Microtubule-Associated Proteins

TRM proteins show a variety of charge profiles (see Supplemental Figure 4 online), and several lack a large basic region reminiscent of the TRM1 microtubule binding domain, suggesting that not all TRM proteins are microtubule-associated proteins. Therefore, five additional members belonging to different subgroups were chosen and fused to GFP to study their localization in tobacco cells. TRM20 and TRM26 displayed a diffuse cytoplasmic staining, whereas GFP fusion of TRM2, TRM8, and TRM25 proteins all decorate microtubule arrays in leaf epidermal cells (Figures 6A to 6F). To confirm their in vivo behavior, TRM8 and TRM26 were tested in cosedimentation assays in vitro. Upon incubation of TRM8 with taxol-stabilized microtubules, TRM8 shifted from the supernatant to the pellet fraction, demonstrating direct association of TRM8 with microtubules (Figure 6G). By contrast, TRM26 remained in the supernatant after incubation with taxol-stabilized microtubules (Figure 6H). Protein charge plot analysis revealed that TRM1, 2, 8, and 25 all possess a large basic domain in their primary sequence, whereas cytoplasmic-localized ones (TRM20 and TRM26) are rather acidic proteins lacking a central basic region (see Supplemental Figure 4 online). No significant sequence similarity is detectable between basic domains of TRM proteins from different subgroups. Based on these results and on protein charge analysis of the whole TRM superfamily, we hypothesize that around half of the TRM proteins are potentially microtubule-associated proteins. This, together with the variety of expression patterns of the 34 TRM genes (see Supplemental Figure 2 online), indicates that the TRM protein superfamily is likely to be involved in a diversity of localization and function in plant cells.

TRM1 Recruits TON1 to Microtubule Arrays

The localization of the GFP-TRM1 fusion as a punctate pattern along microtubules is strongly reminiscent of TON1 localization on cortical microtubule arrays (Azimzadeh et al., 2008). Given the microtubule localization of several TRMs and their ability to interact with TON1 through their M2 motif, TRMs were obvious candidates for TON1's recruitment to cortical microtubule arrays. We tested this hypothesis in planta by transient coexpression of TON1 and TRM1. Overexpression of the GFP-TON1 fusion in *N. benthamiana* leaf cells leads to a diffuse cytoplasmic fluorescence, confirming that TON1 has no ability to bind microtubules by itself (Azimzadeh et al., 2008) (Figure 7A). This also suggests that overproduction of TON1 exceeds the capacity of the cell to localize it properly, maybe due to limitation and/or regulation of the TON1 recruiting machinery in such cells. By contrast, GFP-TRM1 clearly labeled the cortical microtubule network (Figure 7B). Remarkably, coexpression of GFP-TON1 with TRM1-RFP induced redistribution of the GFP-TON1 fluorescence from the cytoplasm to the microtubule network, where it colocalized with TRM1 (Figures 7D to 7F and 7J to 7L). When the same experiments were performed with an M2-deleted version of TRM1 (unable to interact with TON1), TON1-GFP remained in the cytoplasm, while TRM1$^{1-827}$-RFP still localized to microtubules (Figures 7G to 7I). Continuous staining of TRM1 and TON1 along microtubules in this expression system likely reflects an overexpression effect, since when the expression
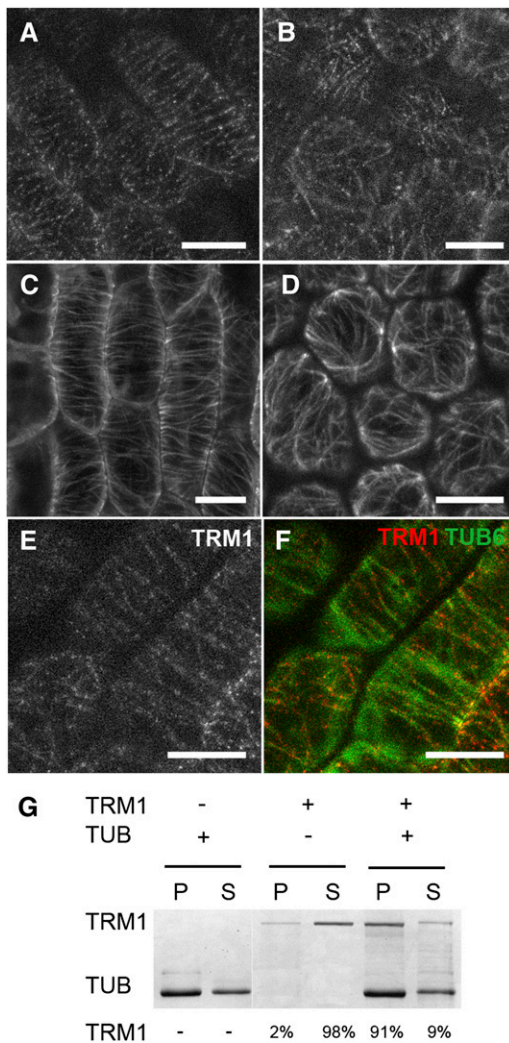
level of both fusions was decreased, punctate localization was observed in *N. benthamiana* cells, in agreement with previous results using stable expression of endogenous promoter-driven fusions (Figures 7M to 7O).

In conclusion, in tobacco leaf epidermal cells, TRM1 is able to target TON1 to the microtubule network via its M2 motif. The recruitment of GFP-TON1 to microtubules by TRM1 in this transient expression assay indicates that microtubule-associated TRMs could be the link between TON1 and cortical microtubule arrays in planta.

C-Terminal Motifs of TRMs Are Present in CAP350, a Human Centrosomal Protein

A human centrosomal proteome (Andersen et al., 2003) was subjected to MAST analysis using the six motifs of *Arabidopsis* TRMs, as previously defined. A significant match was obtained with human CAP350, which contains the three C-terminal motifs M3-M4-M2 in the same configuration as in plant TRMs (Figure 8A), although more distant from one another in this large protein (>3000 residues). CAP350, a large human centrosomal protein (Yan et al., 2006), is responsible for recruitment of FOP at the centrosome. CAP350 is conserved in Holozoa and Chromalveolata but absent in Plantae and Fungi (Hodges et al., 2010). All animal CAP350s possess these three sequence motifs. Although such short and degenerate sequence motifs can generate many false-positive hits in large data sets, their occurrence at conserved positions in all CAP350 proteins, with individual P value scores all below 10^{-4}, and especially in the correct order, is highly significant. Moreover, the M2 motif, defined above as responsible for interaction with TON1, is present within the last 48 C-terminal residues of CAP350 proteins (see Supplemental Figure 5 online), the very same region previously shown in human cells to be involved in interaction with FOP and FOP's recruitment to the centrosome (Yan et al., 2006). In addition, the full-length *Arabidopsis* TON1 was able to interact with the M2 region of human CAP350 in a yeast two-hybrid assay (Figure 8B), confirming the functionality of this region as a bona fide M2 motif.

Remarkably, apart from occurrence of these short sequence motifs, sequence conservation is totally undetectable by standard means between CAP350 and TRMs. Although the N termini of TON1 and FOP clearly have sufficient sequence similarity to infer a common evolutionary origin (Azimzadeh et al., 2008), the occurrence of three motifs of TRM proteins in animal CAP350s is more puzzling and may represent a case of sequence convergence.

DISCUSSION

In our search for TON1-interacting proteins, we identified a novel superfamily of 34 *Arabidopsis* proteins defined by the occurrence of six novel protein motifs. The family shows no extended sequence similarity across all members, but multiple alignment

Figure 4. TRM1 Is a Microtubule-Associated Protein.

(A) to **(F)** GFP-TRM1 labels microtubules in *Arabidopsis* petal epidermal cells. In **(A)** and **(B)**, *Arabidopsis* petal epidermal cells expressing the ProTRM1:GFP-TRM1 construct are shown. In elongated cells from the petal claw **(A)**, GFP-TRM1 fluorescence is present at the cortex as a filamentous labeling organized in parallel arrays perpendicular to the cell elongation axis. In rounded cells from the abaxial side of the petal blade **(B)**, GFP-TRM1 labeled randomly organized cortical filamentous structures. In an *Arabidopsis* mCherry-β-tubulin6 line (**[C]** and **[D]**), the overall cortical microtubule organization in elongated cells from the petal claw **(C)** and in rounded cells from the abaxial side of the petal blade **(D)** is similar to the GFP-TRM1 labeling shown in **(A)** and **(B)**. However, GFP-TRM1 appeared as dots aligned along filaments (**[A]** and **[B]**), whereas mCherry-tubulin is evenly distributed along microtubules (**[C]** and **[D]**). Coalignment of GFP-TRM1 (red) with microtubules (green) was demonstrated in cells coexpressing the ProTRM1:GFP-TRM1 construct and the mCherry-β-tubulin6 marker **(F)**. In **(E)**, the GFP-TRM1 fluorescence alone is shown. **(E)** and **(F)** correspond to petal epidermal elongated cells. All micrographs are projections of Z-stack confocal images. Bars = 10 μm.
(G) TRM1 cosediments with microtubules in vitro. Cosedimentation experiments were performed with 0.5 μM TRM1 in the presence (+) or absence (−) of 0.5 μM microtubules. Proteins present in the supernatant (S) and the pellet (P) after centrifugation were separated on a SDS-PAGE gel stained with Coomassie blue. The intensity of each TRM1 band was measured and expressed as the percentage of the total amount of TRM1 input.
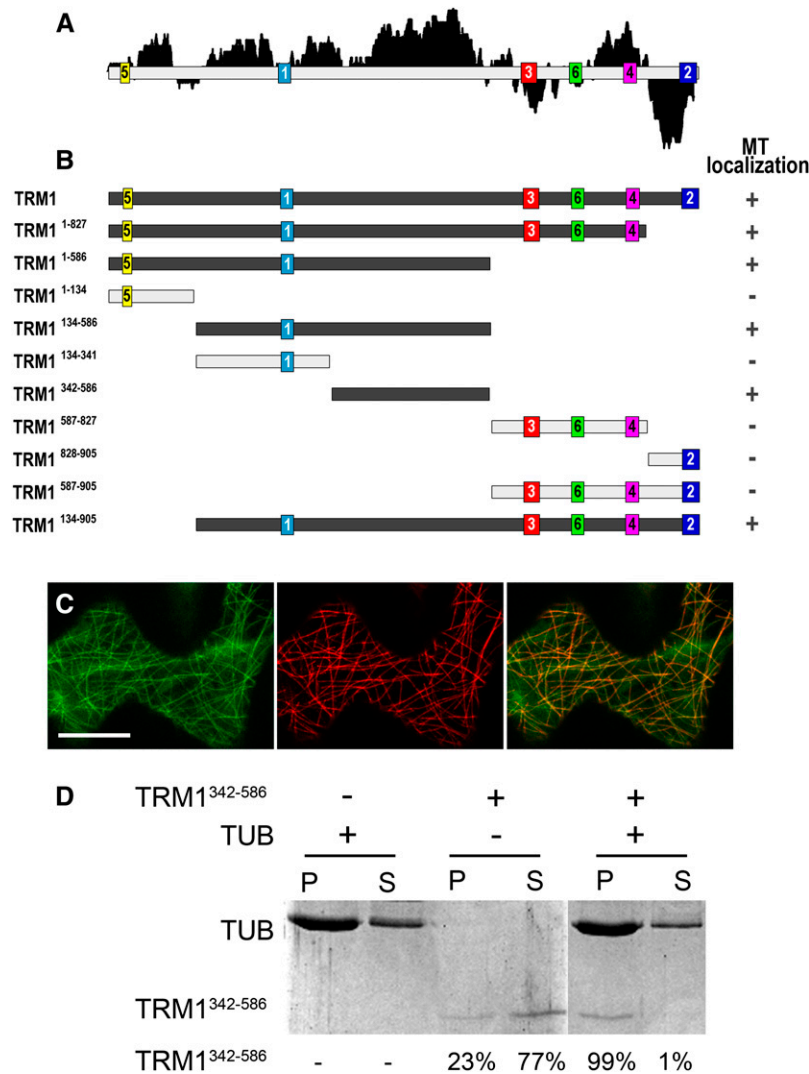
Figure 5. Mapping the TRM1 Microtubule-Interacting Domain.

(A) Schematic representation of TRM1. The position of each motif is indicated. The charge plot of the protein is shown in black, and points above the protein represent positively charged (basic) domains and the ones below negatively charged (acidic) domains.

(B) A series of truncated fragments of TRM1 were cloned in translational fusion with GFP, as N- and C-terminal fusions, under the control of the 35S promoter and expressed transiently in *N. benthamiana* epidermal cells. N- and C-terminal fusions gave comparable results in these experiments. Dark-gray fragments labeled microtubules structures, whereas white ones gave a cytoplasmic staining. MT, microtubule.

(C) Colocalization with microtubules was confirmed by coexpression of the microtubule marker GFP-α-tubulin6 with each TRM1 fragment fused to RFP. An example of such colocalization in *N. benthamiana* jigsaw puzzle leaf cells is shown, where the minimal TRM1$^{342-586}$ fragment (red) colocalized with GFP-α-tubulin6 (green). The right panel corresponds to the overlay of both signals. Bar = 20 μm.

(D) The TRM1$^{342-586}$ binds microtubules in vitro. Cosedimentation experiments were performed with 0.5 μM TRM1$^{342-586}$ in the presence (+) or absence (−) of 0.5 μM microtubules. Proteins present in the supernatant (S) and the pellet (P) after centrifugation were separated on an SDS-PAGE gel stained with Coomassie blue. The intensity of each TRM1$^{342-586}$ band was measured and expressed as the percentage of the total amount of TRM1$^{342-586}$ input.

of TRM sequences allowed us to define several subgroups, within which sequence similarity extends outside the six motifs. We show here that the C-terminal M2 motif of TRM1 is necessary and sufficient for TON1 interaction with TRM1. Given that all 34 *Arabidopsis* TRMs possess an acidic C-terminal tail containing the M2 motif and that 12 TRMs, belonging to almost all similarity groups, were recovered from the yeast two-hybrid interaction screen with TON1, it is likely that all TRMs are to some extent able to bind TON1. Whether they do in the cell or whether other cellular components are able to interact with the M2 region is not known. The other motifs of TRMs could be involved in other types of interactions with other cellular partners. The FASS protein, a PP2A subunit involved in the same pathway as TON1 (Camilleri et al., 2002) that possesses similarity to an animal centrosomal protein (Schlaitz et al., 2007), could be a likely candidate for participating in a same complex with TON1 and TRMs.
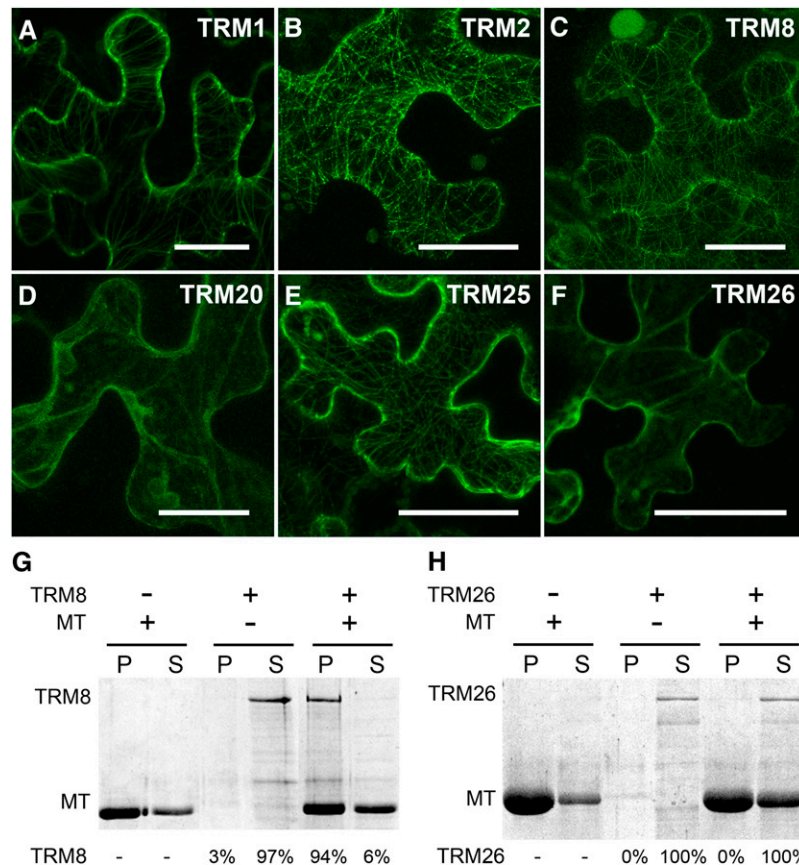
Figure 6. Not All TRM Proteins Are Microtubule-Associated Proteins.

(A) to **(F)** TRM proteins were expressed as N-terminal GFP fusions in *N. benthamiana* leaf epidermal cells. GFP-TRM1 **(A)**, GFP-TRM2 **(B)**, GFP-TRM8 **(C)**, and GFP-TRM25 **(E)** all labeled cortical microtubule arrays, whereas GFP-TRM20 **(D)** and GFP-TRM26 **(F)** displayed a cytoplasmic fluorescence. All micrographs are projections of Z-stack confocal images. Bars = 10 μm.

(G) and **(H)** TRM8 **(G)** and TRM26 **(H)** microtubule (MT) cosedimentation assays. Each cosedimentation was performed with 0.5 μM TRM proteins in the presence (+) or absence (−) of 0.5 μM microtubules. Proteins present in the supernatant (S) and the pellet (P) after centrifugation were separated on an SDS-PAGE gel stained with Coomassie blue. The intensity of each TRM band was measured and expressed as the percentage of the total amount of TRM input. TRM8 directly binds to microtubules in vitro, whereas TRM26 does not.

[See online article for color version of this figure.]

Based on the localization of GFP-TRM1 fusion, colocalization studies, and in vitro binding assays, we established that TRM1 localizes to cortical microtubules arrays via its central basic domain. Many microtubule-associated proteins contain a positively charged basic domain involved in direct interaction with the acidic tails of tubulins (Polakis, 1997; Smith et al., 2001; Culver-Hanlon et al., 2006; Mishima et al., 2007). Charge analysis of TRM primary sequences shows that around half of TRM family members possess such a large basic region (see Supplemental Figure 4 online), indicating that microtubule binding could be a common theme for these TRM proteins. In this study, we confirmed this for TRM2, TRM8, and TRM25. TRMs lacking a large basic domain may represent molecular adapters needed to recruit TON1 and/or other protein complexes onto other cellular structures.

The nonuniform distribution of GFP-TRM1 along the full length of microtubules is intriguing and requires further investigation.

The fact that the GFP-TRM1 fluorescence is faint and only detectable in petals is not favorable to dynamics studies in vivo. In vitro studies of TRM1 localization and dynamics on individual microtubules could prove to be more informative in this respect. Punctate patterns have been observed for several other plant proteins, such as SPR2-GFP (Yao et al., 2008), GFP-CLASP (Ambrose et al., 2007), or MOR1 (Hamada et al., 2004). Punctate patterns along cortical microtubules have also been observed for TON1 (Azimzadeh et al., 2008), consistent with its recruitment by TRM1 to microtubules. Although TON1 was readily described as microtubule associated, this small, acidic protein has presumably no ability to directly interact with microtubules (Azimzadeh et al., 2008). Here, we show that TRM1 directly interacts with microtubules and is able to recruit GFP-TON1 to microtubule arrays in tobacco. This could account for TON1's recruitment to cortical microtubule arrays. However, TON1 recruitment by TRM1 on microtubules is only visible upon co-overexpression
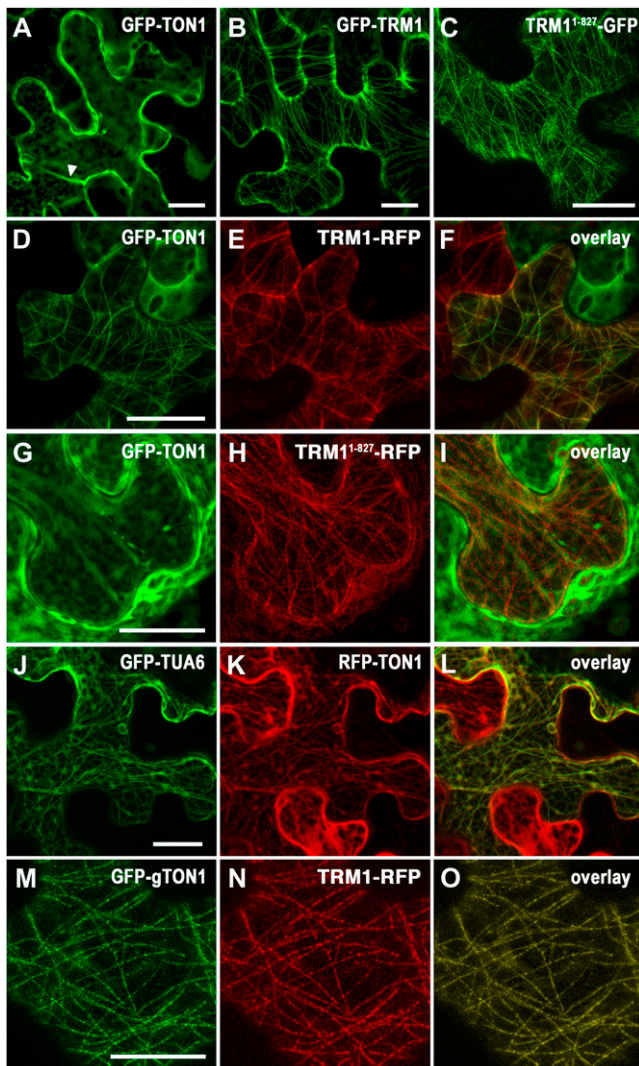
Figure 7. TRM1 Targets TON1 to Microtubules through the TRM1 M2 Motif.

(A) to **(C)** Pro35S-driven expression of GFP-TON1 **(A)**, GFP-TRM1 **(B)**, and TRM1$^{1-827}$-GFP **(C)** in *N. benthamiana* leaf epidermal cells. In these typical jigsaw puzzle cells, the cytoplasm is restricted to the cell's periphery by the large central vacuole penetrated by cytoplasmic strands.

(A) GFP-TON1 fluorescence accumulated diffusely in the cytoplasm and cytoplasmic strands (arrowhead).

(B) and **(C)** GFP-TRM1 and TRM1$^{1-827}$-GFP both labeled microtubule arrays.

(D) to **(I)** Coexpression of GFP-TON1 with TRM1-RFP (**[D]** to **[F]**) or TRM1$^{1-827}$-RFP (**[G]** to **[I]**) in tobacco leaf epidermal cells. Note that the GFP-TON1 signal is recruited to cytoskeletal structures only in cells expressing TRM1 (e.g., in the top right cell in **[D]** to **[F]**), which does not express TRM1-RFP, as judged from lack of RFP fluorescence, and the GFP-TON1 signal remains diffusely in the cytoplasm. In **(G)** to **(I)**, an M2-deleted version of TRM1 (TRM1$^{1-827}$) is unable to recruit GFP-TON1, which remained in the cytoplasm.

(J) to **(L)** Colocalization experiments of RFP-TON1 with the GFP-α-tubulin6 microtubule marker (GFP-TUA6) in tobacco leaf cells. Leaves

of both proteins, which means that endogenous tobacco TRMs are not sufficient to address large amounts of GFP-TON1 to microtubular structures or that the cytoplasmic background is too high to detect such localization. In *Arabidopsis*, the GFP-TON1 fusion weakly labels cortical microtubule structures (Azimzadeh et al., 2008). These are indications that in vivo, the amounts of TRMs and/or their ability to bind TON1 are limited or regulated or that the recruitment of TON1 to the cytoskeleton is transient during the cell cycle and/or differentiation. It is also possible that TRMs that do not localize to microtubules possess the ability to recruit/sequester TON1 to other subcellular compartments. Centrin, which interacts with TON1 (Azimzadeh et al., 2008), and FASS, a PP2A phosphatase subunit (Camilleri et al., 2002), could be involved in regulation of the activity and/or localization of TON1 at the cortex.

Several lines of evidence point to functional diversity among members of the TRM superfamily: (1) Beyond the occurrence of a variable number of short conserved motifs that define the superfamily, the high sequence diversity within the TRM family and the number of subgroups presumably reflects a variety of functions; (2) TRMs display a variety of transcriptional expression patterns. Analysis with the Genevestigator tool (Zimmermann et al., 2004) showed that several TRM genes are expressed throughout plant development, whereas others are induced at specific stages or in specialized tissues (see Supplemental Figure 2 online). In addition, several TRM genes appear to have a cell cycle–regulated expression or to be up- or downregulated under stress conditions (data not shown); (3) genetic analysis of *LNG2/TRM1* and *LNG1/TRM2* genes in a previous study reinforces this assumption. Indeed, these two genes appear to be involved in the control of cell elongation but seem to have no direct role in cell plane positioning and PPB formation (Lee et al., 2006). Thus, it is tempting to speculate that if TRM proteins are part of a molecular pathway involving TON1 and controlling cortical arrays organization, members or subgroups of this superfamily may have acquired specialized functions that cover one or only a few aspects of TON1 functions. For example, focusing on TRM genes upregulated at the beginning or during mitosis could be more relevant to uncover molecular pathways involved in PPB formation in plant cells. Likewise, one or several TRM proteins could be involved in the process of gravity perception, a function recently uncovered for TON1 during functional analysis of this gene in moss (Spinner et al., 2010).

were coinfiltrated with three different constructs: GFP-α-tubulin6, the RFP-TON1 construct, and an untagged version of TRM1. In cells where TRM1 is expressed as revealed by RFP-TON1 recruitment to cytoskeletal structures, the RFP-TON1 signal colocalized with the GFP-α-tubulin6 microtubule marker.

(M) to **(O)** Coexpression of GFP-TON1 and TRM1-RFP at lower expression levels shows a punctate staining reminiscent of TRM1 and TON1 localization in *Arabidopsis*. To decrease expression levels of the TON1 fusion, we used the GFP-gTON1 construct. To decrease expression levels of the TRM1 fusion, agrobacteria carrying the TRM1-RFP construct were resuspended in infiltration buffer to an OD$_{600}$ of 0.05 (instead of 0.5).

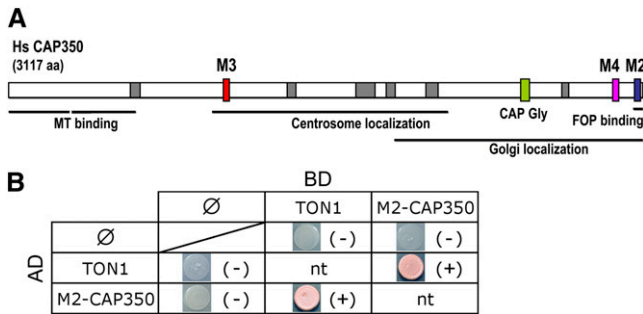All micrographs are projections of Z-stack confocal images. Bars = 20 μm.

Figure 8. The CAP350 M2 Motif Interacts with TON1.

(A) CAP350 proteins contain the M2, M3, and M4 motifs of TRM proteins. Here, a map of human CAP350 where gray boxes indicate coiled-coil regions is shown. Positions of the M3, M4, and M2 motifs are indicated, as well as the CAP-Gly domain of CAP350. Below are regions of CAP350 implicated in microtubule binding, centrosome localization, and interaction with FOP (Yan et al., 2006; Hoppeler-Lebel et al., 2007). This last region corresponding to the C-terminal 48 amino acids of CAP350 coincides precisely with the predicted M2 motif.
(B) The CAP350 M2 motif interacts with TON1. We tested the ability of the C-terminal 48 amino acids of CAP350 to interact with *Arabidopsis* TON1 in a yeast two-hybrid assay: A clear positive interaction was observed, demonstrating the functionality of CAP350 M2 as a TON1 binding motif. ∅, self-activation tests of the constructs; AD, activation domain; BD, binding domain; nt, not tested.
[See online article for color version of this figure.]

The M3, M4, and M2 motifs are present in CAP350, a large centrosomal protein that recruits FOP to the centrosome. The C-terminal M2 motif of CAP350 precisely coincides with the region involved in FOP binding and is recognized by TON1 as a bona fide interaction partner in yeast. In the unicellular alga *Chlamydomonas*, a FOP-like protein is present, distant from land plants' TON1 (Azimzadeh et al., 2008). No bona fide TRM is detected in this species; instead, there is a large coiled-coil protein containing C-terminal M3-M4-M2 motifs. Therefore, *Chlamydomonas* proteins seem closer to animal FOP/CAP350 than to land plants' TON1/TRM, a feature consistent with the presence of a centriole-based MTOC in *Chlamydomonas*. In land plants, TRMs could be functional equivalents at the plant cell's cortex of centrosomal recruiting agents, which in animal centrosomes are mainly large coiled-coil proteins contributing to formation of the pericentriolar matrix and to the recruitment of several protein complexes. In mammalian cells, centrosomes organize interphase and mitotic microtubules networks by controlling nucleation and anchoring processes (Delgehyr et al., 2005). Very little information is available as to whether acentrosomal plant cells have retained, reorganized, or reinvented functions associated with MTOCs in other eukaryotes. The core nucleation proteins of the γ-TurC are clearly conserved in plants and have been extensively studied. Other centrosomal proteins, notably pericentriolar matrix proteins or proteins involved in microtubule anchoring at the centrosome like Ninein, are classically considered absent from plants (Hodges et al., 2010). This view now has to be reconsidered since we have uncovered growing evidences that TON1, FASS, their partners (TRMs), and centrin all have common parts with animal proteins present at the centrosome. One of the

proposed functions for FOP and CAP350 in human cells is microtubule anchoring at the centrosome (Yan et al., 2006). Little molecular information about microtubule anchoring at the plant cell's cortex is available to date, although many observations point to constant and strong connections between the plasma membrane and the cortical cytoskeleton (Dhonukshe et al., 2003). Connections of microtubules with one another, with microfilaments, or with membranes and connections of nucleation centers at the surface of extant microtubules (Murata et al., 2005) could all involve functions reminiscent of microtubule anchoring at the centrosome, involving TRMs and TON1.

METHODS

Plant Material and Growth Conditions

Arabidopsis thaliana plants were grown in vitro or in the greenhouse as described previously (Nacry et al., 1998). *Nicotiana benthamiana* plants were grown in the growth chamber under 16 h of light, a diurnal temperature of 25°C, and a nocturnal temperature of 20°C.

Bioinformatics and Sequence Analysis

Various algorithms and databases were used in the course of this study: BLAST sequence similarity search (Altschul et al., 1990), MEME (Bailey and Elkan, 1994)/MAST (Bailey and Gribskov, 1998) motif analysis and search software, and ClustalW (Thompson et al., 1994), MUSCLE (Edgar, 2004) and MAFFT (Katoh et al., 2005) multiple alignment procedures. The MacVector suite was used for phylogenetic analyses. *Arabidopsis* databases such as SUBA (Heazlewood et al., 2007) were queried for subcellular localization and Arabi-coil (Rose et al., 2004) for coiled-coil segments. We used the complete predicted set of proteins from *Arabidopsis*, rice (*Oryza sativa*), and *Physcomitrella* from TAIR version 9 (http://www.Arabidopsis.org/), Rice Assembly v5 (http://rice.plantbiology.msu.edu/), and *Physcomitrella* v1.1 (http://genome.jgi-psf.org/Phypa1_1/), respectively. Charge plot analysis of protein sequences was performed in Microsoft Excel, calculating the total charge over a sliding window of 51 residues (−1 for D and E, +1 for K and R, and +0.5 for H).

Molecular Cloning Techniques

TRM1 and truncated versions of TRM1, TON1a, TON1b, TRM2, TRM8, TRM20, TRM25, and TRM26 open reading frames were amplified from *Arabidopsis* cDNA clones (Columbia ecotype) using specific primers flanked by AttB1 and AttB2 sites (see Supplemental Table 2 online), cloned into Gateway vector pDONR207 using BP recombination (Invitrogen), and sequenced. The C-terminal 48 amino acids of CAP350 were amplified from the CAP350 cDNA (kind gift of Anne-Marie Tassin, Institut Curie, France) and cloned as above in pDONR207. Expression vectors were obtained after LR recombination (Invitrogen) between these entry vectors and the following destination vectors: pGWB5 and pGWB6 (Nakagawa et al., 2007) for expression of C- and N-terminal GFP fusions, respectively, pH7RWG2 and pH7WGR2 (Van Damme et al., 2004) for expression of C- and N-terminal RFP fusions, respectively, and pDEST17 (Invitrogen) for expression of TRMs in *Escherichia coli*. The ProTRM1:GFP-TRM1 construct was obtained by replacing the p35S promoter of the Gateway destination pB7WGF2 vector (http://www.psb.ugent.be) by the TRM1 promoter (which corresponds here to 2000 bp upstream of the TRM1 ATG start codon). After sequencing, the resulting destination vector was then used in a LR recombination reaction with the TRM1 entry vector.

To obtain the TON1 genomic translational fusion, a 7.4-kb *Pvu*II-*Xho*I genomic fragment containing 4.6 kb of promoter region and the complete

TON1a gene were used. This fragment was previously shown to complement the *ton1* mutant phenotype (Azimzadeh et al., 2008). The GFP was PCR amplified and cloned in phase with the start codon of the TON1a gene (see Supplemental Table 2 online). This construct was then cloned into the pENTR1A Gateway entry vector, and a LR reaction between the resulting vector and the pGWB1 destination binary vector was performed.

Vectors used for yeast two-hybrid interaction assays were a modified pGADT7 vector containing the yeast selectable gene *LEU2* and the GAL4 activation domain fused to the Gateway cassette (attR1-Cm[r]-ccdB-attR2) (kind gift of Katia Marrocco, Institut de Biologie Moléculaire des Plantes, France) and a modified pLex10 bait empty (Jacques Camonis, Institut Curie, France) carrying the yeast-selectable gene *TRP1*. The Gateway cassette (attR1-Cm[r]-ccdB-attR2) was introduced into the *Eco*RI site of the LexA DNA binding domain of pLex10. pLex10- and pGADT7-derived plasmids were used in LR reactions (Gateway) with entry vectors containing TRM1 (full length or truncated), TON1a, or the C-terminal region of CAP350.

Two-Hybrid Assays

The yeast two-hybrid screen of a cDNA library from *Arabidopsis* young siliques (Grebe et al., 2000) with a LexA-TON1b fusion protein was performed as described previously (Azimzadeh et al., 2008).

For proteins interaction assays, the L40 yeast strain was used (*MATa trp1 leu2 his3 ade2 LYS2::lexA-HIS3 URA3::lexA-lacZ*). Yeast samples transformed with each bait construct (along with empty prey vector) were plated on minimal medium lacking Trp, Leu, and His with increasing concentration of 3-amino-1,2,4-triazole (0 to 200 mM) to determine the levels of background self-activation of the *HIS3* gene. The lowest concentration of 3-amino-1,2,4-triazole that inhibits growth was then used to study pairwise interactions in yeast samples containing both bait and prey vectors.

Plant Transformation

Each expression vector was introduced in *Agrobacterium tumefaciens* strain C58C1 (pMP90) by electroporation. Plants were stably transformed as described by Clough and Bent (1998). For transient assays, *Agrobacterium* bacterial cultures were incubated overnight at 28°C with agitation. Each culture was pelleted, washed, and resuspended in infiltration buffer (13 g/L S-medium [Duchefa] and 40 g/L Suc, pH 5.7) to an OD_{600} of 0.5. The inoculum was delivered to the lamina tissue of *N. benthamiana* leaves by gentle pressure infiltration through the lower epidermis. To enhance transient expression of GFP and RFP fusion proteins, the viral suppressor of gene silencing p19 (Voinnet et al., 2003) was coexpressed in *N. benthamiana* leaves. For coinfiltration experiments, equal volumes of the two (or three or four) cultures of OD_{600} of 0.5 were mixed before agroinfiltration.

GFP/RFP Imaging

Tissue was mounted in low-melting-point agarose (0.4% in water) and viewed directly using an inverted Zeiss Observer Z1 spectral confocal laser microscope LSM 710 using a C-Apochromat ×63/1.20 W Corr objective (Carl Zeiss). Fluorescence was recorded sequentially after an excitation at 488 nm (Argon laser) for the GFP and at 561 nm (diode-pumped solid-state laser) for the mCherry. We used a selective band of 493 to 558 nm for the GFP and 578 to 657 nm for the mCherry.

Antibody Generation, Immunoblot Analysis of Plant Extracts, and Coimmunoprecipitation Experiments

Two peptides consisting of amino acids 620 to 631 (DFGIKQDRPSLK) and amino acids 694 to 706 (QSNRGPMKPSSDH) of TRM1 were synthesized, conjugated to KLH, and used to generate rabbit polyclonal antibody (Eurogentec). Affinity-purified antibodies were isolated from

antisera by immunoaffinity chromatography using the *E. coli*–produced TRM1 protein (see below) immobilized on NHS-activated Sepharose 4 Fast Flow resin (GE healthcare) according to the manufacturer's protocols. For protein extraction, plant tissues were ground in liquid nitrogen, homogenized in extraction buffer (0.1 M phosphate buffer, pH 7.4, 150 mM NaCl, 30% (v/v) glycerol, 2.5% caseine, and 0.4% [v/v] Triton X-100) using 3 μL of extraction buffer per mg of tissue, incubated at 4°C for 30 min on a rotating wheel, and centrifuged at 10,000*g* for 15 min to remove cell debris. Casein was added to prevent TRM1 proteins from proteolysis (Hamada et al., 2004; Pacher et al., 2004), and equal volumes of protein extracts (corresponding to equal amounts of fresh tissue weight) were loaded in each lane for immunoblot analysis.

Coimmunoprecipitation experiments were performed starting with 150 mg of tissue using 20 μL of magnetic GFP-TRAP_M kit (Chromotek) according to the manufacturer's instructions, except for the lysis and wash buffers, which were replaced by the extraction buffer described above.

Recombinant Protein, Expression, and Purification

His-TRM proteins were expressed in the *E. coli* Rosetta2(DE3)pLysS strain (Novagen). After induction by 0.5 mM isopropyl-β-D-thiogalactopyranoside, cells were grown for 3 h at 37°C. Cells were resuspended in cold lysis buffer (50 mM HEPES, pH 7.5, 100 mM NaCl, 1% [v/v] Triton X-100, and 1% [v/v] Tween 20) and ruptured by two passes through a French pressure cell (SLM Aminco) at 16,000 p.s.i. Cell lysate was centrifuged at 8,000*g* for 5 min, and inclusion bodies containing pellet were washed four times with the same buffer and four additional times with washing buffer (50 mM HEPES, pH 7.5, and 100 mM NaCl). The final pellet was resuspended in solubilization buffer (50 mM HEPES, pH 7.5, 100 mM NaCl, and 3% [w/v] *N*-lauryl sarcosine) and incubated for 1 h at 4°C. Insoluble material were removed by ultracentrifugation at 4°C for 1 h at 100,000*g*. TRM proteins were refolded by five rounds of dialysis at 4°C for 3 h against dialysis buffer (100 mM NaPi, pH 7.5, 150 mM NaCl, 30% [v/v] glycerol, 0.1% [v/v] Triton X-100, 2 mM $MgCl_2$, and 2 mM 2-mercaptoethanol).

Microtubule Binding Assay

Purified bovine tubulin (Vantard et al., 1994) was assembled in G-BRB80 buffer (BRB buffer: 80 mM PIPES, pH 6.8, 1 mM EGTA, and 1 mM $MgCl_2$ plus 1 mM GTP). For microtubule binding assays, microtubules were assembled from 15 μM tubulin in the presence of 20 μM of taxotere (Sigma-Aldrich) in G-BRB80 supplemented with 1 mM DTT at 37°C for 30 min. Microtubules were then incubated with TRM proteins at 20°C for 20 min and sedimented at 150,000*g* for 20 min at 25°C. Supernatants and pellets were analyzed by SDS-PAGE. To estimate the relative abundance of proteins, gels were scanned using an EPSON GT-9600 scanner. Band intensities were estimated as the volume of optical density per millimeter square of band area using Quantity One software (Bio-Rad) and expressed as the percentage of the total amount of protein input.

Accession Numbers

Sequence data from this article can be found in the Arabidopsis Genome Initiative under the following accession numbers: TON1a, At3g55000; and TON1b, At3g55005. The list of accession numbers for *TRM* genes is included in Figure 2.

Supplemental Data

The following materials are available in the online version of this article.

Supplemental Figure 1. Sequence Logo Representation of the Six Motifs Defined from the 34 TRM Proteins.

Supplemental Figure 2. Gene Expression Analysis of the TRM Superfamily.

AUTHOR CONTRIBUTIONS

S.D., M.G., Y.D., A.C., D.B., and M.P. designed the research. S.D., M.G., Y.D., A.C., S.S., E.D., E.S., D.B., and M.P. performed research. O.G. and M.V. contributed new analytic tools. S.D., M.G., Y.D., A.C., D.B., and M.P. analyzed data. S.D., D.B., and M.P. wrote the article.

REFERENCES

Altschul, S.F., Gish, W., Miller, W., Myers, E.W., and Lipman, D.J. (1990). Basic local alignment search tool. J. Mol. Biol. **215:** 403–410.

Ambrose, J.C., Shoji, T., Kotzer, A.M., Pighin, J.A., and Wasteneys, G.O. (2007). The *Arabidopsis CLASP* gene encodes a microtubule-associated protein involved in cell expansion and division. Plant Cell **19:** 2763–2775.

Andersen, J.S., Wilkinson, C.J., Mayor, T., Mortensen, P., Nigg, E.A., and Mann, M. (2003). Proteomic characterization of the human centrosome by protein correlation profiling. Nature **426:** 570–574.

Azimzadeh, J., Nacry, P., Christodoulidou, A., Drevensek, S., Camilleri, C., Amiour, N., Parcy, F., Pastuglia, M., and Bouchez, D. (2008). *Arabidopsis* TONNEAU1 proteins are essential for preprophase band formation and interact with centrin. Plant Cell **20:** 2146–2159.

Bailey, T.L., and Elkan, C. (1994). Fitting a mixture model by expectation maximization to discover motifs in biopolymers. Proc. Int. Conf. Intell. Syst. Mol. Biol. **2:** 28–36.

Bailey, T.L., and Gribskov, M. (1998). Combining evidence using p-values: Application to sequence homology searches. Bioinformatics **14:** 48–54.

Benschop, J.J., Mohammed, S., O'Flaherty, M., Heck, A.J., Slijper, M., and Menke, F.L. (2007). Quantitative phosphoproteomics of early elicitor signaling in *Arabidopsis*. Mol. Cell. Proteomics **6:** 1198–1214.

Binarová, P., Cenklová, V., Procházková, J., Doskocilová, A., Volc, J., Vrlík, M., and Bögre, L. (2006). Gamma-tubulin is essential for acentrosomal microtubule nucleation and coordination of late mitotic events in *Arabidopsis*. Plant Cell **18:** 1199–1212.

Camilleri, C., Azimzadeh, J., Pastuglia, M., Bellini, C., Grandjean, O., and Bouchez, D. (2002). The *Arabidopsis TONNEAU2* gene encodes a putative novel PP2A regulatory subunit essential for the control of cortical cytoskeleton. Plant Cell **14:** 833–845.

Chan, J., Calder, G.M., Doonan, J.H., and Lloyd, C.W. (2003). EB1 reveals mobile microtubule nucleation sites in *Arabidopsis*. Nat. Cell Biol. **5:** 967–971.

Clough, S.J., and Bent, A.F. (1998). Floral dip: A simplified method for *Agrobacterium*-mediated transformation of *Arabidopsis thaliana*. Plant J. **16:** 735–743.

Culver-Hanlon, T.L., Lex, S.A., Stephens, A.D., Quintyne, N.J., and King, S.J. (2006). A microtubule-binding domain in dynactin increases dynein processivity by skating along microtubules. Nat. Cell Biol. **8:** 264–270.

Delgehyr, N., Sillibourne, J., and Bornens, M. (2005). Microtubule nucleation and anchoring at the centrosome are independent processes linked by ninein function. J. Cell Sci. **118:** 1565–1575.

Dhonukshe, P., Laxalt, A.M., Goedhart, J., Gadella, T.W., and Munnik, T. (2003). Phospholipase d activation correlates with microtubule reorganization in living plant cells. Plant Cell **15:** 2666–2679.

Duroc, Y., Bouchez, D., and Pastuglia, M. (2010). The preprophase band and division site determination in land plants. In The Plant Cytoskeleton, B. Liu, ed (New York: Springer), pp. 145–185.

Edgar, R.C. (2004). MUSCLE: Multiple sequence alignment with high accuracy and high throughput. Nucleic Acids Res. **32:** 1792–1797.

Ehrhardt, D.W., and Shaw, S.L. (2006). Microtubule dynamics and organization in the plant cortical array. Annu. Rev. Plant Biol. **57:** 859–875.

Erhardt, M., Stoppin-Mellet, V., Campagne, S., Canaday, J., Mutterer, J., Fabian, T., Sauter, M., Muller, T., Peter, C., Lambert, A.M., and Schmit, A.C. (2002). The plant Spc98p homologue colocalizes with gamma-tubulin at microtubule nucleation sites and is required for microtubule nucleation. J. Cell Sci. **115:** 2423–2431.

Grebe, M., Gadea, J., Steinmann, T., Kientz, M., Rahfeld, J.U., Salchert, K., Koncz, C., and Jürgens, G. (2000). A conserved domain of the *Arabidopsis* GNOM protein mediates subunit interaction and cyclophilin 5 binding. Plant Cell **12:** 343–356.

Hamada, T., Igarashi, H., Itoh, T.J., Shimmen, T., and Sonobe, S. (2004). Characterization of a 200 kDa microtubule-associated protein of tobacco BY-2 cells, a member of the XMAP215/MOR1 family. Plant Cell Physiol. **45:** 1233–1242.

Heazlewood, J.L., Verboom, R.E., Tonti-Filippini, J., Small, I., and Millar, A.H. (2007). SUBA: The *Arabidopsis* Subcellular Database. Nucleic Acids Res. **35**(Database issue): D213–D218.

Hodges, M.E., Scheumann, N., Wickstead, B., Langdale, J.A., and Gull, K. (2010). Reconstructing the evolutionary history of the centriole from protein components. J. Cell Sci. **123:** 1407–1413.

Hoppeler-Lebel, A., Celati, C., Bellett, G., Mogensen, M.M., Klein-Hitpass, L., Bornens, M., and Tassin, A.M. (2007). Centrosomal CAP350 protein stabilises microtubules associated with the Golgi complex. J. Cell Sci. **120:** 3299–3308.

Jackman, M., Lindon, C., Nigg, E.A., and Pines, J. (2003). Active cyclin B1-Cdk1 first appears on centrosomes in prophase. Nat. Cell Biol. **5:** 143–148.

Katoh, K., Kuma, K., Toh, H., and Miyata, T. (2005). MAFFT version 5: Improvement in accuracy of multiple sequence alignment. Nucleic Acids Res. **33:** 511–518.

Kong, Z., Hotta, T., Lee, Y.R., Horio, T., and Liu, B. (2010). The gamma-tubulin complex protein GCP4 is required for organizing

functional microtubule arrays in *Arabidopsis thaliana*. Plant Cell **22:** 191–204.

Lee, Y.K., Kim, G.T., Kim, I.J., Park, J., Kwak, S.S., Choi, G., and Chung, W.I. (2006). *LONGIFOLIA1* and *LONGIFOLIA2*, two homologous genes, regulate longitudinal cell elongation in *Arabidopsis*. Development **133:** 4305–4314.

Lelièvre, H., Chevrier, V., Tassin, A.M., and Birnbaum, D. (2008). Myeloproliferative disorder FOP-FGFR1 fusion kinase recruits phosphoinositide-3 kinase and phospholipase Cgamma at the centrosome. Mol. Cancer **7:** 30.

Liu, B., Joshi, H.C., Wilson, T.J., Silflow, C.D., Palevitz, B.A., and Snustad, D.P. (1994). Gamma-tubulin in *Arabidopsis*: Gene sequence, immunoblot, and immunofluorescence studies. Plant Cell **6:** 303–314.

Lloyd, C., and Chan, J. (2008). The parallel lives of microtubules and cellulose microfibrils. Curr. Opin. Plant Biol. **11:** 641–646.

Manning, J., and Kumar, S. (2007). NEDD1: Function in microtubule nucleation, spindle assembly and beyond. Int. J. Biochem. Cell Biol. **39:** 7–11.

Mazia, D. (1984). Centrosomes and mitotic poles. Exp. Cell Res. **153:** 1–15.

Mineyuki, Y. (1999). The preprophase band of microtubules: Its function as a cytokinetic apparatus in higher plants. Int. Rev. Cytol. **187:** 1–49.

Mishima, M., Maesaki, R., Kasa, M., Watanabe, T., Fukata, M., Kaibuchi, K., and Hakoshima, T. (2007). Structural basis for tubulin recognition by cytoplasmic linker protein 170 and its autoinhibition. Proc. Natl. Acad. Sci. USA **104:** 10346–10351.

Müller, S., Wright, A.J., and Smith, L.G. (2009). Division plane control in plants: New players in the band. Trends Cell Biol. **19:** 180–188.

Murata, T., Sonobe, S., Baskin, T.I., Hyodo, S., Hasezawa, S., Nagata, T., Horio, T., and Hasebe, M. (2005). Microtubule-dependent microtubule nucleation based on recruitment of gamma-tubulin in higher plants. Nat. Cell Biol. **7:** 961–968.

Nacry, P., Camilleri, C., Courtial, B., Caboche, M., and Bouchez, D. (1998). Major chromosomal rearrangements induced by T-DNA transformation in *Arabidopsis*. Genetics **149:** 641–650.

Nakagawa, T., Kurose, T., Hino, T., Tanaka, K., Kawamukai, M., Niwa, Y., Toyooka, K., Matsuoka, K., Jinbo, T., and Kimura, T. (2007). Development of series of gateway binary vectors, pGWBs, for realizing efficient construction of fusion genes for plant transformation. J. Biosci. Bioeng. **104:** 34–41.

Nakamura, M., Ehrhardt, D.W., and Hashimoto, T. (2010). Microtubule and katanin-dependent dynamics of microtubule nucleation complexes in the acentrosomal *Arabidopsis* cortical array. Nat. Cell Biol. **12:** 1064–1070.

Nakamura, M., and Hashimoto, T. (2009). A mutation in the *Arabidopsis* gamma-tubulin-containing complex causes helical growth and abnormal microtubule branching. J. Cell Sci. **122:** 2208–2217.

Nühse, T.S., Stensballe, A., Jensen, O.N., and Peck, S.C. (2003). Large-scale analysis of in vivo phosphorylated membrane proteins by immobilized metal ion affinity chromatography and mass spectrometry. Mol. Cell. Proteomics **2:** 1234–1243.

Pacher, T.B., Jürgens, G., and Guttenberger, M. (2004). Casein provides protection against proteolytic artifacts. Anal. Biochem. **329:** 148–150.

Paradez, A., Wright, A., and Ehrhardt, D.W. (2006). Microtubule cortical array organization and plant cell morphogenesis. Curr. Opin. Plant Biol. **9:** 571–578.

Pastuglia, M., Azimzadeh, J., Goussot, M., Camilleri, C., Belcram, K., Evrard, J.L., Schmit, A.C., Guerche, P., and Bouchez, D. (2006). Gamma-tubulin is essential for microtubule organization and development in *Arabidopsis*. Plant Cell **18:** 1412–1425.

Pastuglia, M., and Bouchez, D. (2007). Molecular encounters at

microtubule ends in the plant cell cortex. Curr. Opin. Plant Biol. **10:** 557–563.

Polakis, P. (1997). The adenomatous polyposis coli (APC) tumor suppressor. Biochim. Biophys. Acta **1332:** F127–F147.

Popovici, C., Zhang, B., Grégoire, M.J., Jonveaux, P., Lafage-Pochitaloff, M., Birnbaum, D., and Pébusque, M.J. (1999). The t (6;8)(q27;p11) translocation in a stem cell myeloproliferative disorder fuses a novel gene, FOP, to fibroblast growth factor receptor 1. Blood **93:** 1381–1389.

Rose, A., Manikantan, S., Schraegle, S.J., Maloy, M.A., Stahlberg, E.A., and Meier, I. (2004). Genome-wide identification of *Arabidopsis* coiled-coil proteins and establishment of the ARABI-COIL database. Plant Physiol. **134:** 927–939.

Schlaitz, A.L., et al. (2007). The *C. elegans* RSA complex localizes protein phosphatase 2A to centrosomes and regulates mitotic spindle assembly. Cell **128:** 115–127.

Smith, L.G., Gerttula, S.M., Han, S., and Levy, J. (2001). Tangled1: A microtubule binding protein required for the spatial control of cytokinesis in maize. J. Cell Biol. **152:** 231–236.

Spinner, L., Pastuglia, M., Belcram, K., Pegoraro, M., Goussot, M., Bouchez, D., and Schaefer, D.G. (2010). The function of TONNEAU1 in moss reveals ancient mechanisms of division plane specification and cell elongation in land plants. Development **137:** 2733–2742.

Stoppin, V., Vantard, M., Schmit, A.C., and Lambert, A.M. (1994). Isolated plant nuclei nucleate microtubule assembly: The nuclear surface in higher plants has centrosome-like activity. Plant Cell **6:** 1099–1106.

Thompson, J.D., Higgins, D.G., and Gibson, T.J. (1994). CLUSTAL W: Improving the sensitivity of progressive multiple sequence alignment through sequence weighting, position-specific gap penalties and weight matrix choice. Nucleic Acids Res. **22:** 4673–4680.

Torres-Ruiz, R.A., and Jürgens, G. (1994). Mutations in the *FASS* gene uncouple pattern formation and morphogenesis in *Arabidopsis* development. Development **120:** 2967–2978.

Traas, J., Bellini, C., Nacry, P., Kronenberger, J., Bouchez, D., and Caboche, M. (1995). Normal differentiation patterns in plants lacking microtubular preprophase bands. Nature **375:** 676–677.

Van Damme, D., Vanstraelen, M., and Geelen, D. (2007). Cortical division zone establishment in plant cells. Trends Plant Sci. **12:** 458–464.

Van Damme, D., Van Poucke, K., Boutant, E., Ritzenthaler, C., Inzé, D., and Geelen, D. (2004). In vivo dynamics and differential microtubule-binding activities of MAP65 proteins. Plant Physiol. **136:** 3956–3967.

Vantard, M., Peter, C., Fellous, A., Schellenbaum, P., and Lambert, A.M. (1994). Characterization of a 100-kDa heat-stable microtubule-associated protein from higher plants. Eur. J. Biochem. **220:** 847–853.

Voinnet, O., Rivas, S., Mestre, P., and Baulcombe, D. (2003). An enhanced transient expression system in plants based on suppression of gene silencing by the p19 protein of tomato bushy stunt virus. Plant J. **33:** 949–956.

Wang, F., Shi, D.Q., Liu, J., and Yang, W.C. (2008). Novel nuclear protein ALC-INTERACTING PROTEIN1 is expressed in vascular and mesocarp cells in Arabidopsis. J. Integr. Plant Biol. **50:** 918–927.

Wasteneys, G.O., and Ambrose, J.C. (2009). Spatial organization of plant cortical microtubules: Close encounters of the 2D kind. Trends Cell Biol. **19:** 62–71.

Weingartner, M., Criqui, M.C., Mészáros, T., Binarova, P., Schmit, A.C., Helfer, A., Derevier, A., Erhardt, M., Bögre, L., and Genschik, P. (2004). Expression of a nondegradable cyclin B1 affects plant development and leads to endomitosis by inhibiting the formation of a phragmoplast. Plant Cell **16:** 643–657.

Wright, A.J., Gallagher, K., and Smith, L.G. (2009). *discordia1* and

alternative discordia1 function redundantly at the cortical division site to promote preprophase band formation and orient division planes in maize. Plant Cell **21:** 234–247.

Yan, X., Habedanck, R., and Nigg, E.A. (2006). A complex of two centrosomal proteins, CAP350 and FOP, cooperates with EB1 in microtubule anchoring. Mol. Biol. Cell **17:** 634–644.

Yao, M., Wakamatsu, Y., Itoh, T.J., Shoji, T., and Hashimoto, T. (2008). Arabidopsis SPIRAL2 promotes uninterrupted microtubule growth by suppressing the pause state of microtubule dynamics. J. Cell Sci. **121:** 2372–2381.

Zeng, C.J., Lee, Y.R., and Liu, B. (2009). The WD40 repeat protein NEDD1 functions in microtubule organization during cell division in *Arabidopsis thaliana*. Plant Cell **21:** 1129–1140.

Zimmermann, P., Hirsch-Hoffmann, M., Hennig, L., and Gruissem, W. (2004). GENEVESTIGATOR. Arabidopsis microarray database and analysis toolbox. Plant Physiol. **136:** 2621–2632.